A novel broadband bi-mode active frequency selective surface

Yang Xu, Jinsong Gao, Nianxi Xu, Dongzhi Shan, and Naitao Song

Citation: AIP Advances **7**, 055012 (2017); doi: 10.1063/1.4980020
View online: https://doi.org/10.1063/1.4980020
View Table of Contents: http://aip.scitation.org/toc/adv/7/5
Published by the American Institute of Physics

A novel broadband bi-mode active frequency selective surface

Yang Xu,[1,2] Jinsong Gao,[1,2,a] Nianxi Xu,[1] Dongzhi Shan,[1] and Naitao Song[1]
[1]*Key Laboratory of Optical System Advanced Manufacturing Technology, Changchun Institute of Optics, Fine Mechanics and Physics, Chinese Academy of Sciences, Changchun 130033, China*
[2]*University of the Chinese Academy of Sciences, Beijing 100039, China*

(Received 20 November 2016; accepted 30 March 2017; published online 24 May 2017)

A novel broadband bi-mode active frequency selective surface (AFSS) is presented in this paper. The proposed structure is composed of a periodic array of convoluted square patches and Jerusalem Crosses. According to simulation results, the frequency response of AFSS definitely exhibits a mode switch feature between band-pass and band-stop modes when the diodes stay in ON and OFF states. In order to apply a uniform bias to each PIN diode, an ingenious biasing network based on the extension of Wheatstone bridge is adopted in prototype AFSS. The test results are in good agreement with the simulation results. A further physical mechanism of the bi-mode AFSS is shown by contrasting the distribution of electric field on the AFSS patterns for the two working states. [http://dx.doi.org/10.1063/1.4980020]

I. INTRODUCTION

With the sharp increment of the quantity of wireless devices, such as smartphone and Tablet PC, much attention is paid to the notion of Electromagnetic Architecture of building (EAoB). Reconfigurable EAoB can not only greatly improve the security of indoor communication, but also make the spectrum reuse more efficiency. To achieve reconfigurable EAoB, the active frequency selective surface (AFSS) is preferred to use in this field, because of its artificially controllable electromagnetic properties. Thereby, large amounts of researches on AFSS have been carried on in recent years.[1–5] Except for the aforementioned application, AFSS is also utilized in many areas, such as telecommunication and antenna design.[6–8]

As we all known, a remarkable feature of AFSS is the capability that freely controlling the transmission and reflection of electromagnetic wave. In general, there are two ways to achieve that. One way is through changing the positions of working frequency in band-pass curve from center to rising edge.[9–12] In Refs. 9–12, both the PIN diodes and passive band-pass frequency selective surface (FSS) structure are mounted in one side of bearing substrate, and an additional bias circuit is needed in the other side of substrate in order to control the states of diodes. By applying positive and null bias between two ends of bias circuit respectively, the AFSS can achieve the switch function between center and rising edge of pass band. While, the other way is by switching the locations of operating frequency between trailing edge and center of band-stop curve.[13–16] As the additional bias circuit would result in the appearance of unwanted parasitic resonance in frequency response curve, the AFSS structures depicted in Refs. 13–16 are simply composed of PIN diodes and passive band-stop FSS structures. The FSS structures not only act as space filters, but also as bias circuits. A good switch from the center of stop band to trailing edge is obtained. However, no matter which way is adopted, the working bandwidth of AFSS is always small, as the Q value at the rising/trailing edge

[a]gaojs999@163.com

is very bad. To obtain high Q value, the AFSS structure should operate at the center of pass band and stop band.

In this paper, a novel broadband bi-mode AFSS structure working at the WLAN band of 2.45GHz for TE and TM polarizations is presented. This structure consists of a periodic array of convoluted square patches and Jerusalem Crosses, with two adjacent Jerusalem Crosses connected to each other by a PIN diode. Based on simulation results, the AFSS structure definitely shows the mode switch between band-pass and band-stop modes with a broad fractional bandwidth. To ensure the accuracy of simulation, a prototype AFSS utilizing a novel bias network is fabricated and tested for both TE and TM polarizations. The test results in agreement with the simulations prove the fact that the broadband bi-mode switch of AFSS can be achieved by controlling the states of PIN diodes, opening up an opportunity for many practical applications, such as radar stealth, telecommunication and antennas design.

II. MODEL AND ANALYSIS

As shown in Fig. 1(a), the composite array of metallic patches, such as cross dipoles and metal squares, can provide the band-stop response. While, in Fig. 1(b), when the adjacent cross dipoles are connected to each other, an array of square loop slots is formed, which means the generation of band-pass response.[17] Inspired by this, we propose to connect the two ends of the adjacent cross dipoles depicted in Fig. 1(a) by PIN diodes. When PIN diodes stay in the ON state, the array of cross dipoles turns into a metallic mesh shown in Fig. 1(b), and therefore an array of square loop slots is obtained. The center wavelength of pass band is close to the perimeter of square loop slot.[12] For PIN diodes in OFF state, except the mutual capacitance between adjacent cross dipoles, extra reverse capacitance of PIN diodes should be considered, which causes that the center wavelength of stop band is much larger than that of pass band. In order to ensure the center wavelengths of pass band and stop band are consistent, we increase the electric resonant length of pass band by utilizing convoluted square loop slot, which would not affect the center wavelength of stop band. Based on the aforementioned design guidelines, a novel AFSS structure which can achieve an excellent switching effect between band-pass and band-stop modes in the frequency range we concerned is provided.

The two-dimensional layout of this 2 x 2 array of AFSS is shown in Fig. 2. Periodic array of metallic convoluted square patches and Jerusalem Crosses connected to each other by PIN diodes on a thin polyimide substrate constitute the AFSS. Every patch is surrounded by four Jerusalem Crosses and they form a convoluted square loop together when the PIN diodes are forward biased. The Jerusalem Crosses not only serve as a biasing circuit in design of AFSS, but also a part of filtering structure.

P is the periodic space of the unit cell, w represents the width of the crossed dipole composing Jerusalem Cross, l_1 denotes the length of the Jerusalem Cross, a_1 and b_1 are the width and length of the end loading of Jerusalem Cross, l_2 is the spacing of the end loadings arranged face to face in a whole Jerusalem Cross, a_2 and b_2 are the width and length of the small rectangular patch noted in Fig. 2, s is the width of the convoluted looped slot and t is the thickness of polyimide substrate with relative dielectric constant of 3 and loss tangent of 0.005.

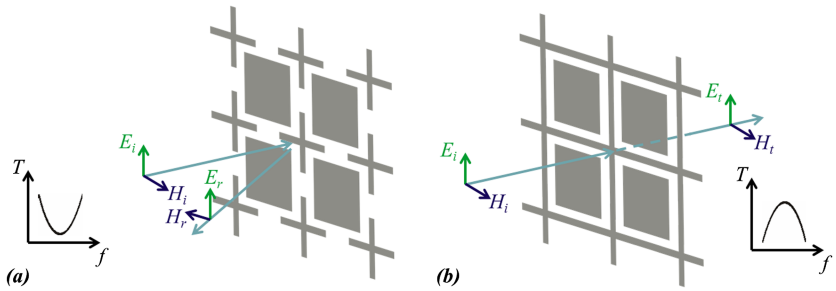

FIG. 1. The schematic diagrams of band-stop (a) and band-pass (b) responses.

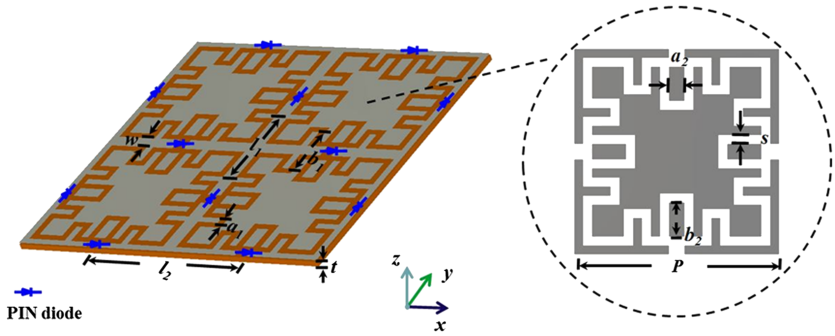

FIG. 2. Two-dimensional sketch of the 2 x 2 array.

On account of the symmetry of unit cell in x label and y label, the frequency response of this AFSS for both TE and TM polarization are same when it's exposed to the normal incidence in free space environment. In order to carry out qualitative analysis better, the frequency response of AFSS exposed to normal incidence can be explained effectively in terms of the equivalent circuit model.[18] Fig. 3 are the simple models and corresponding equivalent circuits of AFSS in ON and OFF states.

For ON state, the parallel LC circuit (L_1 and C_1) shunted across a transmission line means that there is a resonant frequency f_1 with band-pass performance in the frequency response curve. On the contrary, the AFSS in OFF state can be equal to a series LC circuit (L_2 and C_2) in parallel with the capacitance C_3, which indicates the occurrence of two resonances. One resonant frequency f_2 is mainly determined by inductance L_2 together with capacitance C_2, corresponding to the band-stop response. The other resonant frequency f_3 dominantly arises from the inductance L_2 in parallel with capacitance C_3, which cause a band-pass response. Thereby, when the resonant frequency f_1 is close to the resonant frequency f_2, the switch effect between band-pass and band-stop modes at the same frequency can be achieved in AFSS design.

Further analysis of the AFSS structure is performed through utilizing CST software in order to prove the correctness of the thought fore-mentioned. The transmission spectrum of AFSS is acquired by a straightforward coupling of EM simulation and circuit simulation called EM/Circuit Co-Simulation. In EM/Circuit Co-Simulation, the EM simulation based on the finite element method gives the simulation results of passive FSS first. Then, on the basis of results obtained by the former simulation, the total simulation results of AFSS can be indicated by the further SPICE-based circuit simulation. The dimensions of the unit cell are as follows: P=25.3mm, w=2.2mm, l_1=23.5mm,

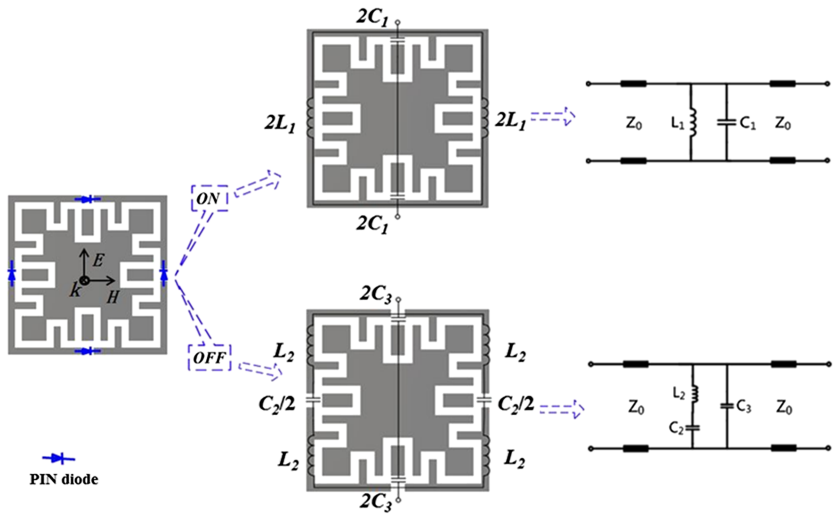

FIG. 3. Simple models and corresponding equivalent circuits of AFSS in ON and OFF states.

TABLE I. Electrical characteristics of the diode.

Type	BAR88-02V	Package	SC79
Item		Symbol	Typ. Values
Forward Voltage		V_f	0.75V
Forward Resistance		R_f	1.5Ω
Reverse Capacitance		C_r	0.28pF
Reverse Resistance		R_r	1.5kΩ

l_2=15.6mm, a_1=1.1mm, b_1=9mm, a_2=1.9mm, b_2=4.2mm, s=1.1mm and t=0.0254mm. The type and parameters of PIN diode adopted in the simulation are depicted in Table I.

The frequency response of AFSS for ON and OFF states under normal incidence is manifested as follows. As described in Fig. 4, the results of EM/Circuit Co-Simulation and equivalent circuit model are in accordance with each other, except the discrepancy of transmission coefficients at center frequency, which is caused by the absence of PIN diode's impedances as well as the loss tangent of the substrate. The transmission spectrum founded on equivalent circuit model is achieved by adjusting the values of capacitance and inductance depicted in Fig. 3 in ADS circuit simulation until the S-parameters of the circuit models coincide with the results from CST software. The characteristic parameters are as follows: C_1=0.564pF, L_1=7.761nH, C_2=0.549pF, L_2=7.495nH and C_3=0.729pF.

From the result of EM/Circuit Co-Simulation, a mode switch between band-pass and band-stop modes close to 2.45GHz is actually achieved for the AFSS under normal incidence by biasing the PIN diodes. When the diodes stay in forward bias state, the frequency response with band-pass

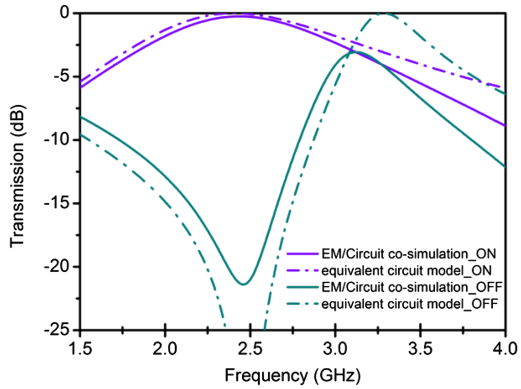

FIG. 4. Frequency response obtained from EM/Circuit co-simulation and predicted by equivalent circuit model of the AFSS structure for ON and OFF state.

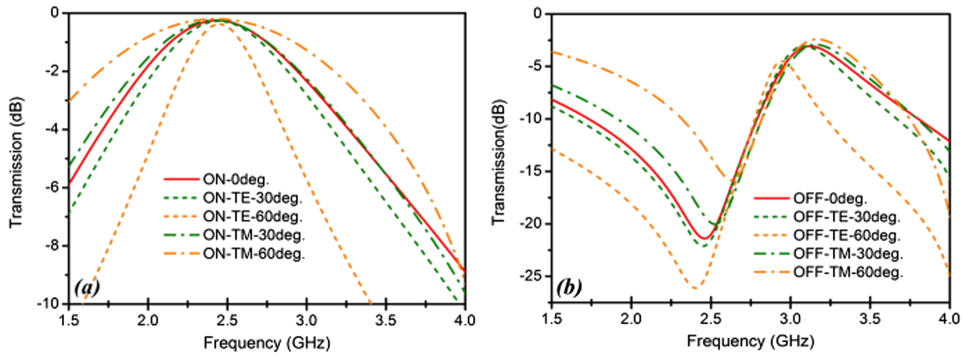

FIG. 5. Frequency response of the AFSS in (a) ON and (b) OFF states with various incident angles for both TE and TM polarizations.

performance emerges at 2.436GHz. While for the situation of the diodes in null bias state, a band-stop response with the center frequency of 2.476GHz is formed. The transmission performances of the AFSS in ON and OFF states at various incident angles for TE and TM polarizations are provided in Fig. 5. As illustrated in Fig. 5(a) and Fig. 5(b), no matter in ON or OFF state, the center frequency of AFSS for both TE and TM polarizations stabilize in the vicinity of 2.45GHz except a minute frequency shift with respect to the incident angle, which would have a very slight effect on the mode switch. Moreover, on account of adopting the convoluted pattern, the AFSS structure also obtain a broadband filtering behavior for both ON and OFF states.[19–21]

III. FABRICATION AND MEASUREMENTS

Although the AFSS structure are well performed according to the aforementioned simulation results, the difficulty that how to apply a uniform bias to each PIN diode is not considered. To resolve such problem in practical fabrication, an ingenious bias network is designed based on the extension of Wheatstone bridge, as shown in Fig. 6.

Similar to Wheatstone bridge, the bias network can also ensure a uniform bias distribution. Besides that, the bias network can infinitely extend along the feeder, meaning a potential in large area application.

Adopting the novel bias network, the prototype AFSS shown in Fig. 7(a) was fabricated by using standard printed circuit board photography and surface-mount technology. The prototype of

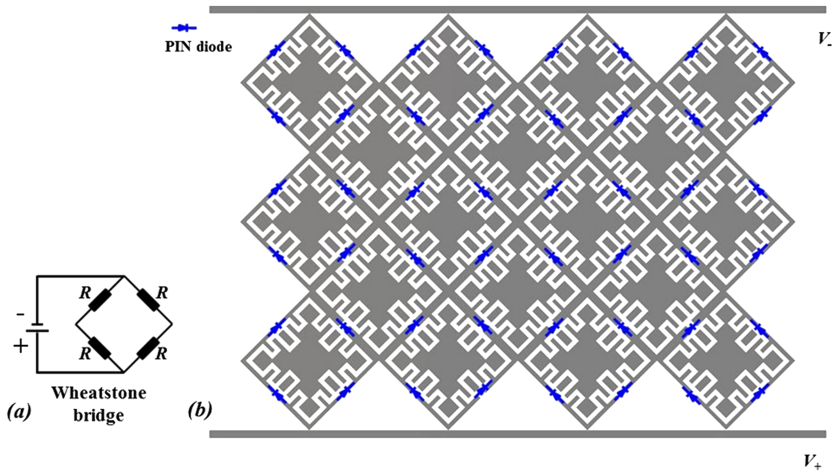

FIG. 6. The schematic diagrams of (a) Wheatstone bridge and (b) the bias network of AFSS.

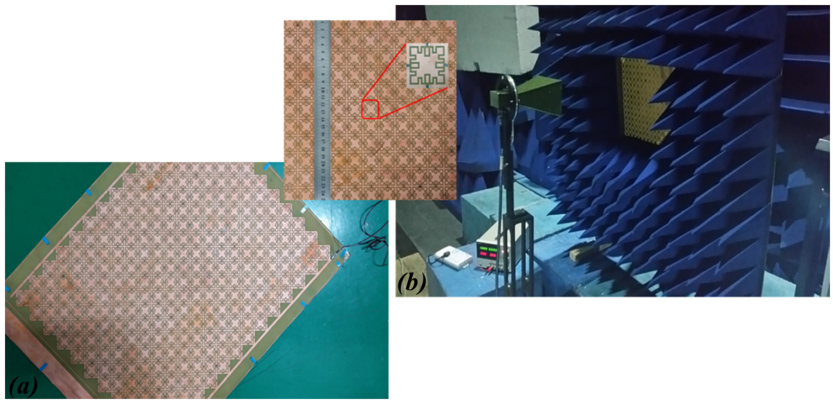

FIG. 7. Photograph of (a) the fabricated AFSS structure and (b) measurement system.

400mm x 500mm incorporates a total of 284 elements. A total dc bias voltage of 18 volts was required for the AFSS of ON state, while in the OFF state, no bias was applied.

As shown in Fig. 7(b), a plane-wave chamber equally divided by a microwave absorber loaded rotatable screen constituted the measurement set-up, thus enabling the angle of incidence transmission measurements to be possible. In the center of screen, a square aperture accepting the prototype under test was placed. A pair of pyramidic horn antennas and an Agilent N5244A vector network analyzer were employed for the transmission system. The testing for both polarizations was achieved by rotating the horn antennas 90°.

IV. RESULTS AND DISCUSSION

The test results of prototype AFSS in ON and OFF states at various incident angles from 0° to 60° are respectively shown in Fig. 8 (a) and (b). By comparing the test results with simulation results, we find that both of them are similar with each other in the same case, except that there is an approximate 300MHz blue shift at the resonant frequency, which may be mostly ascribed to the SPICE model of diodes not containing the package in simulation. Furthermore, fabrication tolerance and the impact of soldering material should not be ignored. As the periodic space of elements (P=25.3mm) is about 1/5 resonant wavelength (λ_0~122mm), namely miniaturized element, a broadband bi-mode switch is obtained and the concrete parameters are shown as follows: -1dB fractional bandwidth of AFSS in ON state and -10dB fractional bandwidth of AFSS in OFF state are respectively 23.3% and 26.3%. Anyway, this experiment positively verifies the accuracy of the analysis in the previous sections.

To better understand the physical mechanisms of the bi-mode AFSS, the electric field distribution on the AFSS patterns for ON and OFF states at 2.45GHz under normal incidence are respectively represented in Fig. 9(a) and Fig. 9(b).

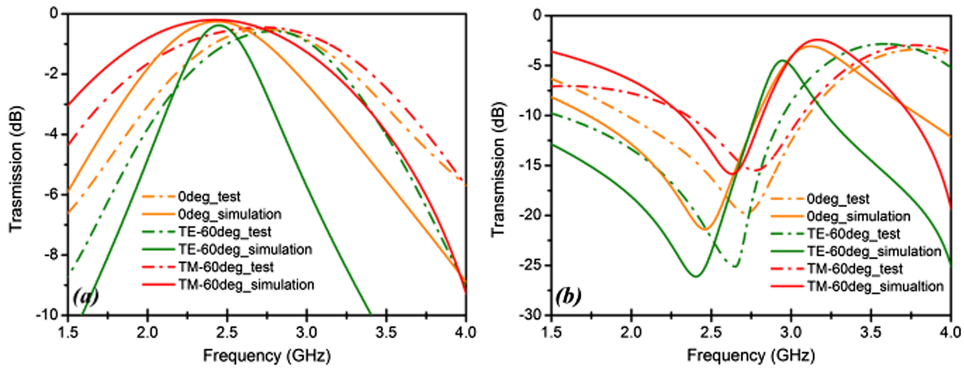

FIG. 8. Comparison between simulation results and test results of the prototype AFSS in (a) ON and (b) OFF states.

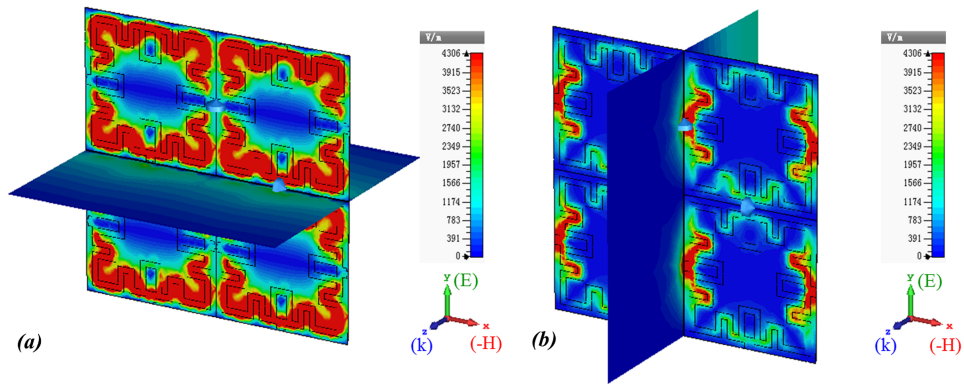

FIG. 9. Distribution of electric field on the AFSS patterns for TE polarization under normal incidence in ON (a) and OFF (b) state at the resonant frequency.

As shown in Fig. 9(a), when the diodes are forward biased, the electric field is mostly distributed in the convoluted loop slot along x direction for TE polarization. This kind of field distribution means that the majority of electric field energy would easily pass through the AFSS structure just like penetrating air. Thus, the AFSS structure in ON state performs the band-pass mode. In contrast, from the Fig. 9(b), we can discover that the electric field mainly focuses on the two ends of the Jerusalem Cross along y direction for TE polarized wave, when the diodes are applied by null bias. This kind of resonance analogous to the radiation of electrical dipole ultimately leads to a strong reflection and therefore the band-stop mode is developed. Due to the structural symmetry of the unit cell, the same answer will be obtained for TM polarization.

V. CONCLUSION

In this paper, we present a novel broadband AFSS structure which can achieve a bi-mode switch between band-pass and band-stop modes at the WLAN band of 2.45GHz. Because of using miniaturized elements in structural design, the AFSS structure can obtain a broadband and stabilized frequency response with various incident angles from 0^o to 60^o for both ON and OFF states, according to the simulation results. In order to verify the correctness of our analysis and simulation, a prototype using an ingenious bias network is fabricated and measured. The test results well coincide with the simulation results, which manifest that the broadband bi-mode switch of AFSS can be easily realized by controlling the states of PIN diodes as we expect. Distribution of electric field on AFSS patterns further explains the physical mechanisms of AFSS structure in ON and OFF states. With excellent filtering ability, this broadband bi-mode AFSS possess an enormous potential in applications of radar stealth, telecommunication and antennas design.

ACKNOWLEDGMENTS

This work is supported by the National Natural Science Foundation of China (Grant No.61172012).

[1] D. Ferreira, I. Cuiñas, R. F. S. Caldeirinha, and T. R. Fernandes, IET Microw. Antenna P **10**, 435–441 (2016).
[2] H. Fabian-Gongora, A. E. Martynyuk, J. Rodriguez-Cuevas, and J. I. Martinez-Lopez, IEEE Microw. Wirel. Co. **25**, 606–608 (2015).
[3] F. Deng, X. J. Xi, J. Li, and F. Ding, IEEE Antenn. Wirel. Pr. **14**, 630–633 (2015).
[4] C. Yang, H. Li, Q. Cao, and Y. Wang, Microw. Opt. Techn. Let. **58**, 535–540 (2016).
[5] W. Hu, M. Y. Ismail, R. Cahill, J. A. Encinar, V. F. Fusco, H. S. Gamble, D. Linton, R. Dickie, N. Grant, and S. P. Rea, Eletron. Lett. **43**, 744–745 (2007).
[6] M. Roig, M. Sazegar, Y. Zheng, and R. Jakoby, *The 7th German Microwave Conference, March 2012*, pp. 1–4.
[7] L. Zhang, G. Yang, Q. Wu, and J. Hua, IEEE T. Magn. **48**, 4534–4537 (2012).
[8] L. Zhang, G. Yang, and Q. Wu, *IEEE Antennas and Propagation Society International Symposium, July 2012*, pp. 1–2.
[9] G. I. Kiani, K. L. Ford, L. G. Olsson, and K. P. Esselle, IEEE T. Antenn. Propag. **58**, 581–584 (2010).
[10] B. Sanz-Izquierdo, E. A. Parker, and J. C. Batchelor, IEEE T. Antenn. Propag. **59**, 2728–2731 (2011).
[11] K. Chang, I. K. Sang, and Y. J. Yoon, *IEEE Radio and Wireless Symposium, Jan. 2008*, pp. 663–666.
[12] G. I. Kiani, K. P. Esselle, A. R. Weily, and K. L. Ford, *IEEE Antennas and Propagation Society International Symposium, June 2007*, pp. 4525–4528.
[13] P. S. Taylor, E. A. Parker, and J. C. Batchelor, IEEE T. Antenn. Propag. **59**, 3265–3271 (2011).
[14] B. Sanz-Izquierdo and E. A. Parker, IEEE T. Antenn. Propag. **62**, 764–771 (2014).
[15] K. Elmahgoub, F. Yang, and A. Z. Elsherbeni, Progress In Electromagnetics Research C **35**, 135–145 (2013).
[16] J. Li, J. Jiang, Y. He, W. Xu, M. Chen, L. Miao, and S. Bie, IEEE Antenn. Wirel. Pr. **15**, 774–777 (2016).
[17] B. A. Munk, *Frequency Selective Surfaces: Theory and Design* (Wiley, New York, 2000).
[18] N. Xu, J. Gao, J. Zhao, and X. Feng, AIP Adv. **5**, 077157 (2015).
[19] E. A. Parker, A. N. A. El Sheikh, and A. C. Lima, IEE Proc. H **140**, 378–380 (1993).
[20] E. A. Parker and A. N. A. El Sheikh, IEE Electron. Lett. **27**, 322–323 (1993).
[21] B. Sanz-Izquierdo, E. A. Parker, J. B. Robertson, and J. C. Batchelor, IEEE Trans Antennas Propag. **58**, 690–696 (2010).